



EPTT-2022-0036

DYNAMICS OF FLUID-SOUND WAVES INTERACTION IN A CFB RISER WITH CALCIUM OXIDE PARTICLES AND AIR WITH CO₂

Sarah Laysa Becker

Federal University of Santa Catarina (UFSC), Reitor João David Ferreira Lima University Campus, Florianópolis - SC, Brazil
University of Blumenau (FURB), São Paulo St. 3250, Blumenau - SC, Brazil
sarahlaysia@gmail.com

Vivien Rossbach

Federal University of Santa Catarina (UFSC), Reitor João David Ferreira Lima University Campus, Florianópolis - SC, Brazil
University of Blumenau (FURB), São Paulo St. 3250, Blumenau - SC, Brazil
vivienrossbach@gmail.com

Henry França Meier

University of Blumenau (FURB), São Paulo St. 3250, Blumenau - SC, Brazil
meier@furb.br

Natan Padoin

Federal University of Santa Catarina (UFSC), Reitor João David Ferreira Lima University Campus, Florianópolis - SC, Brazil
natan.padoin@ufsc.br

Cíntia Soares

Federal University of Santa Catarina (UFSC), Reitor João David Ferreira Lima University Campus, Florianópolis - SC, Brazil
cintia.soares@ufsc.br

Abstract. *Circulating fluidized bed is a great equipment to process solids in post combustion CO₂ capture. It enhances particles distribution, promoting phase contact, adsorption, and reaction. Fluidization of particles can be difficult to achieve, depending on flow and solid characteristics. Based on this, different investigations of intrusive and non-intrusive alternatives to avoid agglomerates, core-annulus profile, and back-mixing are found in the literature. This study aims to investigate the multiphase turbulence of the gas-solid flow of calcium oxide with air and CO₂ in a CFB applying ultrasound waves to improve solids dispersion. It was carried out by CFD simulations employing a URANS-k-ε-KTGF-EMMS model. Results of volume fraction, velocity, pressure drop, Péclet, and dispersion coefficient were evaluated with and without ultrasounds. Acoustic waves change solids velocity and volume fraction profiles along the riser height. Pressure drop increases near the transducers, since they act as flow resistance, but drops above them, becoming lower when compared with the case without acoustics. Solids radial Péclet number also increases near the ultrasound device and the dispersion coefficient decreases, showing that solids dispersion is improved in the region responsible for the first contact between phases. Results reveal the necessity of more investigation about increasing the number of transducers.*

Keywords: *Circulating Fluidized Bed, Multiphase Turbulence, Fluid-Sound Waves Interaction, Computational Fluid Dynamics.*

1. INTRODUCTION

The combustion of fossil fuels, responsible for much of the primary energy supply, results in a significant contribution to the emission of CO₂ into the atmosphere. Despite the efforts to reduce the use of these fuels, it is much likely that they will dominate the energy supply in the coming decades (Jacobson, 2009). Carbon capture is an alternative to reduce CO₂ emissions. It separates CO₂ from the flue gas, stores or transforms it into another product, keeping away from the atmosphere. Post-combustion capture has considerable advantages over the pre-combustion and oxy-fuel combustion techniques since its implementation avoids substantial process modifications. However, the high costs of the carbon capture and storage steps cause a slow deployment of these schemes in industries. Therefore, developing a technique that is economically efficient is a priority in studies of this area (Kanniche *et al.*, 2010).

Solid particles applied to capture CO₂ in adsorption or reaction are a promising alternative due to the low energy consumption. The circulating fluidized bed (CFB) is an excellent equipment for this, since it can process large quantities

of particles. It has advantages over the fixed bed because it enables high heat and mass transfer between phases (Wang *et al.*, 2010). Although, some particles can be difficult to fluidize, depending on characteristics such as diameter, density, and cohesiveness. In high gas velocities, the appearance of agglomerates and/or clusters of particles is common, also the development of solid back-mixing and the core-annulus profile.

Back-mixing regions appear when there is a downward flow of solids and a high velocity upward flow of gas, building a recirculation region (Namkung and Kim, 1998). It is caused by the turbulent flow in the riser, increases erosion (Parsi *et al.*, 2014), affects phase contact and reactions between them (Shi *et al.*, 2015). The core-annulus is a condition in which particles move to the riser wall, forming a dilute region in the center. It affects the solid distribution and the gas-solid contact, harming heat and mass transfer and operations as adsorption and reaction (Gidaspow *et al.*, 2004).

The agglomerates and clusters of particles and the core-annulus profile are investigated in the literature to develop techniques to minimize their effects and improve solids distribution. There are intrusive techniques, as ring baffles (Rossbach *et al.*, 2019) and gas and solid distributors (Peng *et al.*, 2011) that require internal modifications in geometries, and also non-intrusive ones, such as the application of acoustic waves, studied in fluidized beds by Raganati *et al.* (2014) and in CFB risers by Rossbach *et al.* (2021). The acoustic waves directed to gas-solid flows produce a pressure perturbation, changing gas velocity, breaking these agglomerates and the core-annulus profile, enhancing processes that depend on phase contact.

In this context, this study aims to investigate, by computational fluid dynamics (CFD) simulations, the ultrasound waves applied in radial direction to a gas-solid flow in a CFB riser. Calcium oxide and a mixture of air with 10% CO₂ form the solid and the gas phases, respectively. Indeed, these particles (CaO) are largely used in CO₂ capture and the percentage of CO₂ (10%) is common in flue gases used in post-combustion capture processes. In this previous study reactions were disregarded.

2. MATHEMATICAL MODEL

The mathematical model applied to represent gas-solid flow in a CFB riser was a transient Eulerian-Eulerian approach, in which both phases were treated as continuous and interpenetrating. This phenomenon involves the conservation of mass, momentum, species, and energy to consider the gas as a compressible fluid.

The interfacial forces between phases, summarized in the drag force, were modeled by Energy Minimization Multi-Scale (EMMS) proposed by Yang *et al.* (2003). EMMS stands out due to its potential to represent the dilute flows, the cluster formation, and the core-annulus profile, adding a transition function to the model for high gas volume fraction conditions. The effect of collisions between particles was obtained using the Kinetic Theory of Granular Flow (KTGF). This model introduces and calculates the variable solids pressure in the momentum equations. KTGF was also used to obtain the granular temperature and the turbulent viscosity (Alves and Mori, 1999).

The standard k-ε model of Jones and Launder (1972) was employed to model turbulence of the gas phase. The turbulent viscosity was obtained by Eq. (1) with additional transport equations.

$$\mu_{t,g} = \rho_g C_\mu \frac{k_g^2}{\varepsilon_g} \quad (1)$$

in which ρ_g is the gas density, k_g is the turbulent kinetic energy, ε_g its dissipation, and C_μ an empirical constant with the value suggested by the authors of 0.09. Moreover, the Enhanced Wall Treatment (EWT) was employed in the regions near the walls. This approach combines the k-ε with wall functions, improving its results in the viscous sub-layer. The turbulent Reynolds number was calculated to separate the mesh in two regions: the turbulent one, in the center of domain, in which the k-ε model was applied, and another region near the walls calculated by the EWT, where viscous forces dominate (Wolfshtein, 1969). The turbulence interaction was used to describe momentum transfer between continuum and disperse phases. It is calculated using the model of Simonin and Viollet (1990b). Furthermore, turbulent dispersion evaluated by Simonin and Viollet (1990a) was implemented to calculate drift velocity.

The acoustic model enforced to describe the effects of ultrasonic waves on the air was based on the acoustic pressure produced by the transducers. Lighthill (1978) acoustic streaming model represents the excess pressure over the hydrostatic pressure in the wave propagation direction as:

$$P_{ex} = \rho_g c_0 u_0 \cos[\omega(t - x/c)] \quad (2)$$

where c is the phase velocity (m/s), u_0 the acoustic wave velocity (m/s), ω is the angular frequency (rad/s), and t is time (s). Sajjadi *et al.* (2015), based on Lighthill (1978), introduced the compression-rarefaction effect in the equations and became it independent of the position (x):

$$P(t) = -P_a \sin(\omega t) \quad (3)$$

in which P_a is the acoustic pressure ($P_a = \sqrt{2\rho_g I_{US} c_0}$) and I_{US} is the ultrasound intensity, expressed as the ratio between input power of the transducers and transducer's face area.

3. METHODOLOGY

CFD simulations of gas-solid flow were performed in a tridimensional circulating fluidized bed with a simplified geometry presented in Fig. 1. It consists of a cylindrical riser with 2.667 m in height and 104 mm in diameter, with a pipe bend on the top. The gas inlet was at the bottom of the riser. Solid particles were fed by an adjacent pipe with 44 mm of diameter in 0.4 m of riser height with 45° of inclination. The outlet is located after the pipe bend, in the top of the geometry. Solids inlet and riser outlet have an inclination of 12°. The ultrasound device intended to enhance solids distribution was positioned between 0.63 m and 0.70 m in height. It is composed of 20 transducers divided into four vertical lines, positioned in the x-direction, orthogonal to the solids inlet, and y-direction, parallel to this (Fig. 1a).

The CFB riser geometry presented in Fig. 1a was discretized as a non-uniform block structured mesh, divided into 525,534 elements. Figure 1b illustrates the discretization. It is possible to observe that, in the regions of solids inlet and ultrasound device, the mesh was refined.

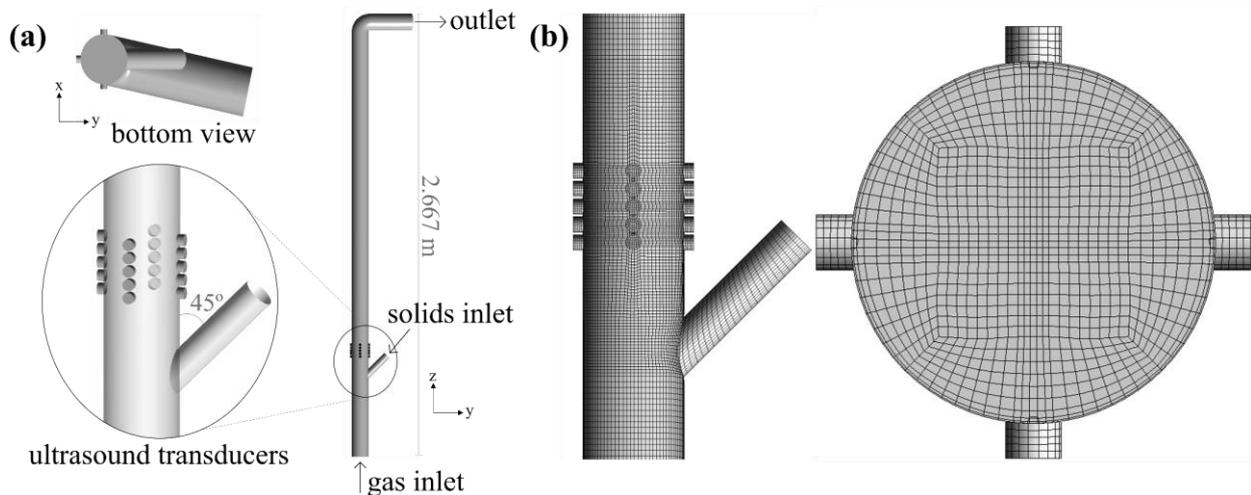


Figure 1. CFB riser: (a) geometry; and (b) mesh views and highlights.

Air with 10% of carbon dioxide and calcium oxide were used as gas and solid phases, respectively. The gas flows through the pipe with a velocity of 8.8 m/s. It was implemented in the simulations as an outlet boundary condition of -8.8 m/s, to give the effect of the exhauster equipment employed in the real experimental unit, that was positioned after the outlet. More information about the experimental CFB riser is available in Rossbach *et al.* (2021). The calcium oxide particles used as solid phase have a diameter of 100 μm and 3320 kg/m^3 of density. They enter solids inlet with a mass flow rate of 0.0249 kg/s .

About the ultrasound device, mechanical waves were delivered at the transducers' faces as pressure waves, consistent with the Sajjadi's model in Eq. (3). These mechanical waves mimic the effect of the acoustic waves in the fluid. Thus, it was considered that all the acoustic momentum was converted into fluid dynamics momentum. The attenuation of the acoustic energy in the fluid was deemed in the Navier-Stokes equations. A user-defined function (UDF) was applied in the simulations to represent the acoustic waves in each transducer's face. The configurations of the ultrasound device were selected based on Rossbach *et al.* (2020). The sound frequency selected was 20 kHz, with a sound pressure level of 120 dB and a power intensity of 10 W. At the walls, no-slip and free-slip conditions were established for gas and solid phases, respectively.

Simulations were carried out with and without ultrasound waves at ambient conditions of temperature and pressure. Mathematical modelling introduced in the previous section were employed in the simulations with the aid of ANSYS Fluent 19.1. Ten seconds of simulation were got in the two cases to analyze the mean results. About the numerical solutions, the pressure-velocity coupling was estimated with Phase-Coupled SIMPLE scheme. The convergence criteria of 10^{-4} and a variable time-step between 10^{-5} and 10^{-4} s were chosen.

Besides solids volume fraction, solids velocity and pressure drop, results of radial Péclet number and dispersion coefficient were analyzed. For particle diffusion, Péclet is defined as the product of Reynolds and Schmidt numbers. It correlates the convective and diffusive effects of gas-solid dispersion and it is employed to measure radial solids dispersion in the CFB riser. Radial Péclet was calculated by the correlation of Wei *et al.* (1998) for circulating fluidized beds by the Eq. (4).

$$Pe_{sr} = 225.7(1 - f_s)^{-0.29}Re_t^{0.43} \quad (4)$$

This correlation employs the turbulent Reynolds number (Re_t) and the mean solids volume fraction (f_s) of the cross section obtained in the simulations.

The solid volume fraction dispersion coefficient was employed based on Rossbach *et al.* (2021) methodology. It represents the statistical covariance of the distribution of solids volume fraction, and it was calculated as the ratio between the standard deviation ($\bar{\sigma}_{sd}$) and the mean solids volume fraction (\bar{f}_s) at the cross-section of the riser by the Eq. (5).

$$C_v = \bar{\sigma}_{sd}/\bar{f}_s \quad (5)$$

4. RESULTS AND DISCUSSION

Fluid dynamics results of the numerical simulations of gas-solid flow in the circulating fluidized bed are evaluated in this section. Solids volume fraction, solids velocity, pressure drop, and radial Péclet number are analyzed as contours, volume renderings, and profiles.

Contours of mean solid volume fraction in different riser heights are illustrated in Fig. 2 with and without ultrasounds. They are positioned in the center of each transducer row (0.629 m, 0.647 m, 0.666 m, 0.684 m, and 0.703 m) and above the ultrasound device (0.75 m, 1.00 m, 1.25 m, 1.50 m, 1.75 m). Comparing them, results without acoustic waves show particles enter and flow through the riser accumulated on the opposite side of the inlet, near the wall, as can be seen in the contours of Fig. 2b. With ultrasounds, contours in the device demonstrate the effect of the transducers. Solids are more distributed over the cross section (Fig. 2a). Above the transducers, particles tend to accumulate near the wall, forming a profile similar to the core-annulus.

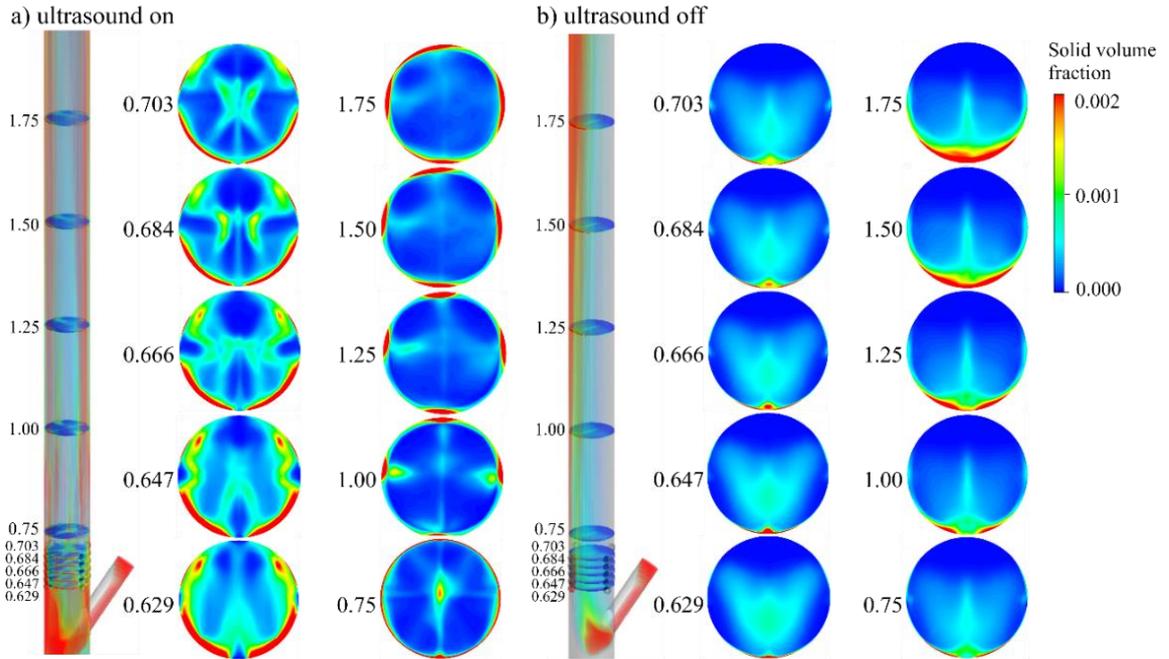


Figure 2. Contours and volume rendering of mean solids volume fraction: (a) with ultrasound waves; and (b) without ultrasound waves.

Moreover, the mean solids volume fraction and velocity profiles are evaluated in x- and y-axis, being x orthogonal to the solids inlet and y parallel to this, as exhibited in Fig. 3 and 4. Profiles are showed in 0.66 m, in the middle of the ultrasound device, and above it (0.75 m, 1.00 m, 1.25 m, 1.50 m, and 1.75 m) with the volume rendering of this part of the geometry. Results are compared with and without ultrasounds.

Evaluating solids volume fraction, results without acoustic waves in y-direction present a maximum in the negative radius, close to the wall (Fig. 3b), agreeing with the contours. On the opposite side, in the positive radius, the volume fraction is really close to zero. Therefore, there is almost no particle flow. This confirms that solids flow through the riser accumulated on the opposite side of the inlet. In the x-axis, without ultrasounds, the profile is smooth, with a slightly higher concentration near the walls.

Implementing the ultrasound device in the CFB unit makes solid volume fraction profile smoother in 0.66 m in x- and y-directions (Fig. 3a). Above the transducers, solids seem to accumulate near the walls, in consonance with the contours of Fig. 2a.

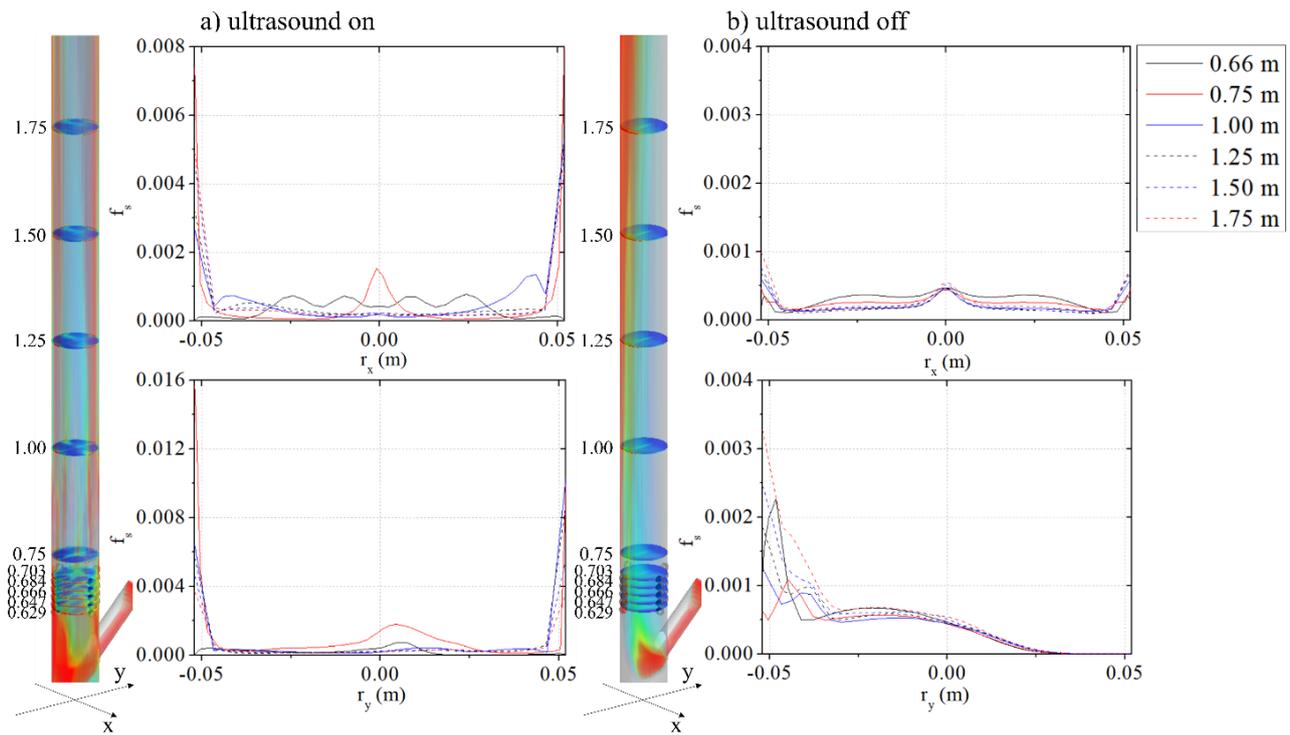


Figure 3. Mean solids volume fraction volume rendering and profile in x- and y-axis: (a) with ultrasound waves; and (b) without it in 0.66 m, 0.75 m, 1.00 m, 1.25 m, 1.50 m, and 1.75 m of height.

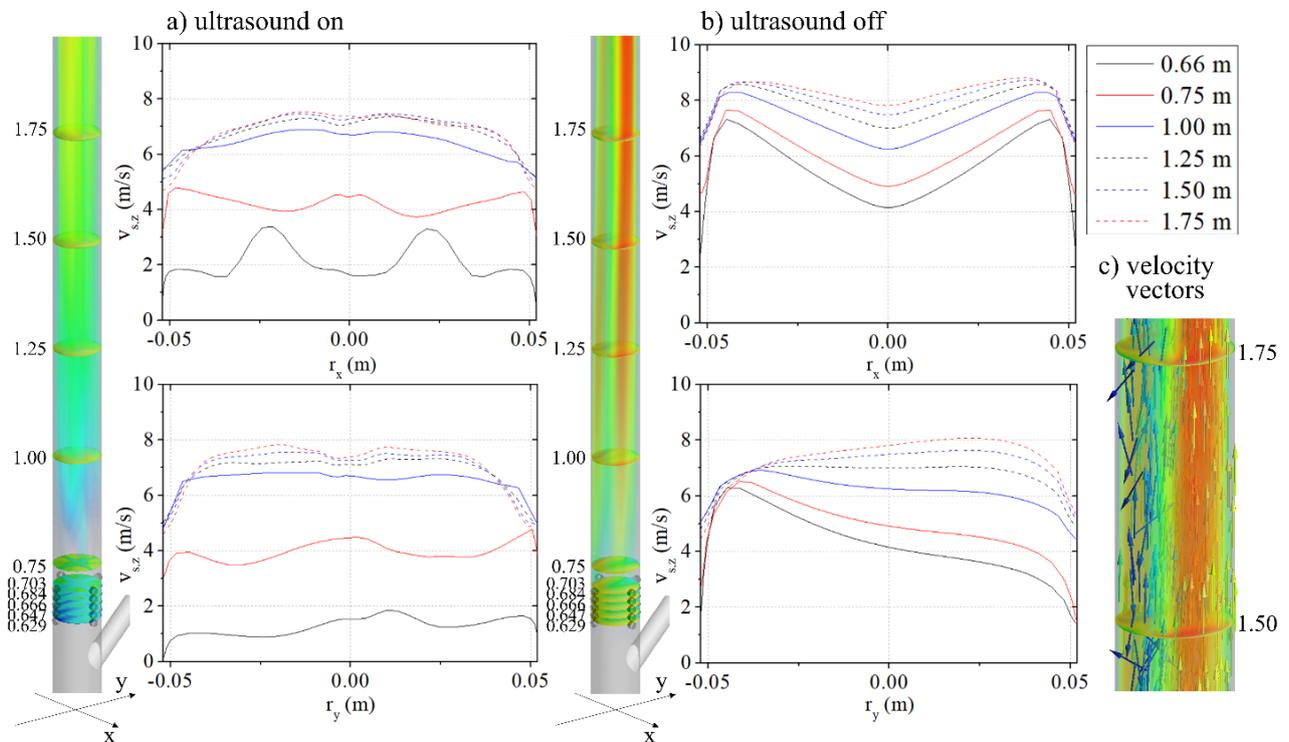


Figure 4. Mean solids velocity volume rendering and profile in x- and y-axis (a) with; (b) without ultrasound waves in 0.66 m, 0.75 m, 1.00 m, 1.25 m, 1.50 m, and 1.75 m of height; and (c) a highlight of solid velocity vectors in 10.82 s of simulation.

The profiles of mean solid velocity are depicted in Fig. 4 with its volume rendering. Indeed, the acoustic waves smooths the profile in both directions. In the y-axis, without ultrasounds, two different profiles are observed (Fig. 4b).

Velocity profile has a maximum in the negative radius (left side), where the major part of solids is flowing in 0.66 m, 0.75 m and 1.00 m of height. Above 1.00 m, particles appear to spread a little in the riser cross section and the profile changes. In contrast, the right side (+r_y), in which solids volume fraction is lower, has the highest velocity. Since the amount of solids is small, they are easily transported by the gas and almost reach its velocity. In the left side, where are most part of the solids, the velocity drops, which can indicate particle drop or back-mixing.

The back-mixing is a condition caused by turbulence in the riser, in which particles drop a little and flow up with the gas, creating a recirculation region. To emphasize, the Fig. 4c exhibits solids velocity vectors in 10.82 s, that demonstrates particles flow direction. It is possible to note a recirculation region on the left side of the riser, which corresponds to the back-mixing. This problem is avoided by using the ultrasound device, as illustrated in Fig. 4a. With acoustic waves, the velocity profile becomes more uniform, with higher velocity in the center of the pipe and lower near the walls. This is probably due to of the particles accumulated in the walls, showed in the volume fraction contours (Fig. 2a).

These results indicate that acoustic waves assist solids dispersion, change the solids volume fraction and velocity profiles in all the pipe height. However, analyzing the volume fraction, a smooth profile is exhibited only in the position of 0.66 m, in the middle of the ultrasound device. We can conclude that results can be improved by increasing the number of transducers.

Pressure drop, radial Péclet number, and solids dispersion coefficient are analyzed along the riser height in Fig. 5. Mean values were taken from cross section planes in the middle of each transducers row (0.629 m, 0.647 m, 0.666 m, 0.684 m, and 0.703 m) and above them (0.75 m, 1.00 m, 1.25 m, 1.50 m, 1.75 m, 2.00 m, 2.25 m, and 2.50 m).

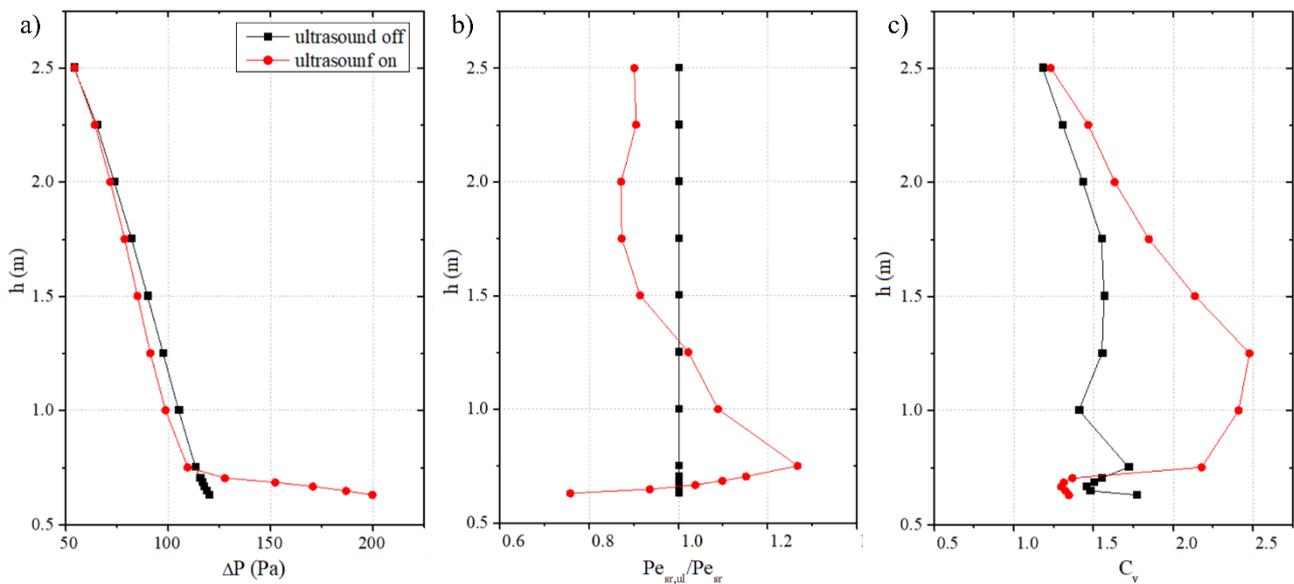


Figure 5. Mean pressure drop along the riser height (a); solids radial Péclet number with ultrasounds normalized by the Péclet without it (b); and solids volume fraction dispersion coefficient (c).

Figure 5a corresponds to the mean pressure drop along the CFB riser with and without acoustic waves. It relates the pressure in the analyzed plane with the pressure in the outlet since an exhaustor is used to flow gas. Comparing them, the pressure drop is higher near the transducers in the case with ultrasound on. This is the region where Sajjadi *et al.* (2015) model is applied. It acts on the pressure field and changes particles velocity, causing a cross flow in the region near the transducers, that behaves as an upward flow resistance. This occurs because the model does not consider acoustic dissipation, transferring all the acoustic energy into mechanical energy. It is also noted that the acoustic waves cause particle drop in the region above the solids inlet due to this flow resistance generated in the transducers.

Meanwhile, the pressure drop decreases along the transducers (Fig. 5a), since acoustic energy is converted to kinetic energy and it is aggregated to the gas-solid flow. Beyond the ultrasound device region, the pressure drop along the riser height is close with and without acoustic waves. The case with ultrasounds presents a lowest pressure drop. It probably happens in this case because ultrasounds prevent the appearance of back-mixing. Without it, the energy of the flow is insufficient to carry solid particles, enhancing pressure drop.

Figure 5b illustrates solids radial Péclet number with acoustic waves normalized by Péclet without it ($Pe_{sr,ul}/Pe_{sr}$). The simulation with ultrasound off is represented by a narrow line (Pe_{sr}/Pe_{sr}). The Péclet should increase to indicate that the solids dispersion has improved. In transducers region, this dimensionless number increases and keeps higher until 1.25 m. Above it, Péclet reduces in relation to the case without acoustic waves. The highest Péclet values are observed in the first meter of riser height, which shows that gas-solid dispersion is enhanced there. This region is right above the solids inlet, responsible for the first contact between phases, and, in reactive flows, it is where chemical reactions begin.

Overall, these results also reveal the necessity of install more transducers at the riser height, that could be installed at 1.25 m, where Péclet reduces.

Finally, the solids volume fraction dispersion coefficient, showed in Fig. 5c, was calculated for both simulations. The mean value of solids volume fraction in 1200 points of the cross-section planes at different riser heights was employed. For the dispersion coefficient, the lower its value, more homogeneous the distribution of particles in the cross-section. Results show that near the transducers, C_v is lower in the case with acoustic waves. This confirms that ultrasounds enhance solids distribution. However, above them, the dispersion coefficient increases, reaching its peak at 1.25 m. Over this point, C_v reduces, being close to the case without ultrasounds in the riser's top. In other words, dispersion is improved by the ultrasound but becomes worse above it. This behavior can be related to the high concentration of solids, in which flow kinetic energy is not enough to maintain radial dispersion. Near the transducers, the turbulent flow causes particle collisions and kinetic energy loss, so there is no sufficient energy to disperse particles in the region above it. This can be seen in the formation of the core-annulus profile after the transducers.

In summary, this low influence of acoustic waves over the solids dispersion can be associated also with the acoustic wave frequency applied and the size of the particles. Waves of 20 kHz can capture particles with diameter around $7.25 \mu\text{m}$ in its pressure nodes (Rossbach *et al.* 2021). In this study, calcium oxide particles have $100 \mu\text{m}$. Despite this, the ultrasound really affects particles trajectory, improving dispersion in transducers region.

5. CONCLUSIONS

The investigation of the fluid dynamics of gas-solid flow in a circulating fluidized bed with acoustic waves applying calcium oxide particles with air and CO_2 was concluded by CFD simulations. The mathematical modelling URANS-k- ϵ -KTGF-EMMS represented this multiphase turbulent flow inside the CFB riser with the model of Sajjadi *et al.* (2015) to achieve the acoustic pressure in the ultrasound device.

Profiles, contours, and volume renderings of mean solids volume fraction revealed that the acoustic waves change particle distribution throughout the riser height, improving it in the transducers' region. Without ultrasounds, solids were accumulated near the wall, on the opposite side of the inlet. Applying ultrasounds, the profile in the transducer's region became smoother, and, above it, solids flow near the walls, with a core-annulus profile.

The mean solids velocity profiles were also analyzed, with the volume rendering and the velocity vectors. Results highlighted a back-mixing region observed in y-direction, on the left side of the riser. It was caused by the accumulation of particles flowing in this turbulent region. It can be avoided by using the ultrasound device, which makes the velocity profile more uniform.

The mean pressure drop along the riser height increased 42.32% in the transducers' region (0.629 m until 0.703 m) with acoustic waves. It was caused by the appliance of Sajjadi's model that perform as a flow resistance. Above them, pressure drop with acoustic waves became 3.63% lower when compared with the other case, probably because ultrasounds prevented the appearance of back-mixing. In the case without acoustics, pressure drop was enhanced because the flow energy was not enough to rise solid particles.

Furthermore, solids radial Péclet number was evaluated with and without ultrasounds. It was possible to note that Péclet increased near the transducers and kept high until 1.25 m. This demonstrates that solids dispersion was improved by the ultrasound in the inlet region, where the first contact between phases occurs and the reactions begin. Above it, results revealed a reduction of radial Péclet number.

Lastly, the solids volume fraction dispersion coefficient was calculated and evaluated by comparing simulations. In the region of the ultrasound device, the dispersion coefficient showed excellent results, with values 13.87% lower in the case with ultrasounds. This is in line with the Péclet number results, demonstrating that ultrasound improved particle distribution in this region.

In conclusion, the results showed that particle distribution was improved in the transducers' region. Despite the change in solids velocity profile, the back-mixing disappeared, the pressure drop was lower with acoustic waves, and the distribution was not enhanced above the transducers. It can be related to the number of transducers that can be increased, and the sound frequency applied. It reveals the necessity of further investigations in this regard.

6. ACKNOWLEDGEMENTS

The authors are grateful for the financial support of Coordination for the Improvement of Higher Education Personnel (CAPES) – Process number 88887.495480/2020-00.

7. REFERENCES

Alves, J.J.N. and Mori, M., 1999. "Analyses of parametric sensitivity in the kinetic theory of granular flows on the prediction of the fluid dynamics of circulating fluidized bed reactors". *Computers & Chemical Engineering*, Vol. 23, p. 757-760.

- Gidaspow, D., Jung, J., and Singh, R. K., 2004. "Hydrodynamics of fluidization using kinetic theory: an emerging paradigm". *Powder Technology*, Vol. 148, p. 123-141.
- Jacobson, M.Z., 2009. "Review of solutions to global warming, air pollution, and energy security". *Energy & Environmental Science*, Vol. 2, p. 148-173.
- Jones, W.P. and Launder, B.E., 1972. "The prediction of laminarization with a two-equation model of turbulence". *International Journal of Heat and Mass Transfer*, Vol. 15, p. 301-314.
- Kanniche, M., Gros-Bonnivard, R., Jaud, P., Valle-Marcos, J., Amann, J.M., and Bouallou, C., 2010. "Pre-combustion, post-combustion and oxy-combustion in thermal power plant for CO₂ capture". *Applied Thermal Engineering*, Vol. 30, p. 53-62.
- Lighthill, S., 1978. "Acoustic streaming". *Journal of Sound and Vibration*, Vol. 61, p. 391-418.
- Namkung, W. and Kim, S. D., 1998. "Gas backmixing in a circulating fluidized bed". *Powder Technology*, Vol. 99, n. 1, p. 70-78.
- Parsi, M., Najmi, K., Najafifard, F., Hassani, S., Mclaury, B. S., and Shirazi, S. A., 2014. "A comprehensive review of solid particle erosion modeling for oil and gas wells and pipelines applications". *Journal of Natural Gas Science and Engineering*, Vol. 21, p. 850-873.
- Raganati, F., Ammendola, P., and Chirone, R., 2014. "CO₂ adsorption on fine activated carbon in a sound assisted fluidized bed: effect of sound intensity and frequency, CO₂ partial pressure and fluidization velocity". *Applied Energy*, Vol. 113, p. 1269-1282.
- Rossbach, V., Utzig, J., Decker, R.K., Noriler, D., Soares, C., Martignoni, W.P., and Meier, H.F., 2019. "Gas-solid flow in a ring-baffled CFB riser: numerical and experimental analysis". *Powder Technology*, Vol. 345, p. 521-531.
- Rossbach, V., Padoin, N., Meier, H.F., and Soares, C., 2020. "Influence of acoustic waves on the solids dispersion in a gas-solid CFB riser: numerical analysis". *Powder Technology*, Vol. 359, p. 292-304.
- Rossbach, V., Padoin, N., Meier, H.F., and Soares, C., 2021. "Influence of ultrasonic waves on the gas-solid flow and the solids dispersion in a CFB riser: numerical and experimental study". *Powder Technology*, Vol. 389, p. 430-449.
- Sajjadi, B., Raman, A.A.A., and Ibrahim, S., 2015. "Influence of ultrasound power on acoustic streaming and micro-bubbles formations in a low frequency sono-reactor: mathematical and 3D computational simulation". *Ultrasonics Sonochemistry*, Vol. 24, p. 193-203.
- Simonin, O. and Viollet, P.L., 1990. "Modeling of Turbulent Two-Phase Jets Loaded with Discrete Particles". *Phenomena in Multiphase Flows*, p. 259-269.
- Simonin, O. and Viollet, P.L., 1990. "Predictions of an Oxygen Droplet Pulverization in a Compressible Subsonic Coflowing Hydrogen Flow". *Numerical Methods for Multiphase Flows*, p. 65-82.
- Shi, X., Sun, R., Lan, X., Liu, F., Zhang, Y., and Gao, J., 2015. "CPFD simulation of solids residence time and back-mixing in CFB risers". *Powder Technology*, Vol. 271, p. 16-25.
- Wang, W., Lu, B., Zhang, N., Shi, Z., and Li, J., 2010. "A review of multiscale CFD for gas-solid CFB modeling". *International Journal of Multiphase Flow*, Vol. 36, p. 109-118.
- Wei, F., Cheng, Y., Jin, Y., and Yu, Z., 1998. "Axial and lateral dispersion of fine particles in a binary-solid riser". *The Canadian Journal of Chemical Engineering*, Vol. 76, p. 19-26.
- Wolfshtein, M., 1969. "The velocity and temperature distribution in one-dimensional flow with turbulence augmentation and pressure gradient". *International Journal of Heat and Mass Transfer*, Vol. 12.
- Yang, N., Wang, W., Ge, W., and Li, J., 2003. "CFD simulation of concurrent-up gas-solid flow in circulating fluidized beds with structure-dependent drag coefficient". *Chemical Engineering Journal*, Vol. 96, p. 71-80.

8. RESPONSIBILITY NOTICE

The authors are the only responsible for the printed material included in this paper.